

YMTHE, Volume 27

## **Supplemental Information**

### **Improving mRNA-Based Therapeutic Gene Delivery**

**by Expression-Augmenting 3' UTRs Identified**

**by Cellular Library Screening**

**Alexandra G. Orlandini von Niessen, Marco A. Poleganov, Corina Rechner, Arianne Plaschke, Lena M. Kranz, Stephanie Fesser, Mustafa Diken, Martin Löwer, Britta Vallazza, Tim Beisert, Valesca Bukur, Andreas N. Kuhn, Özlem Türeci, and Ugur Sahin**

# **Supplementary Material and Methods**

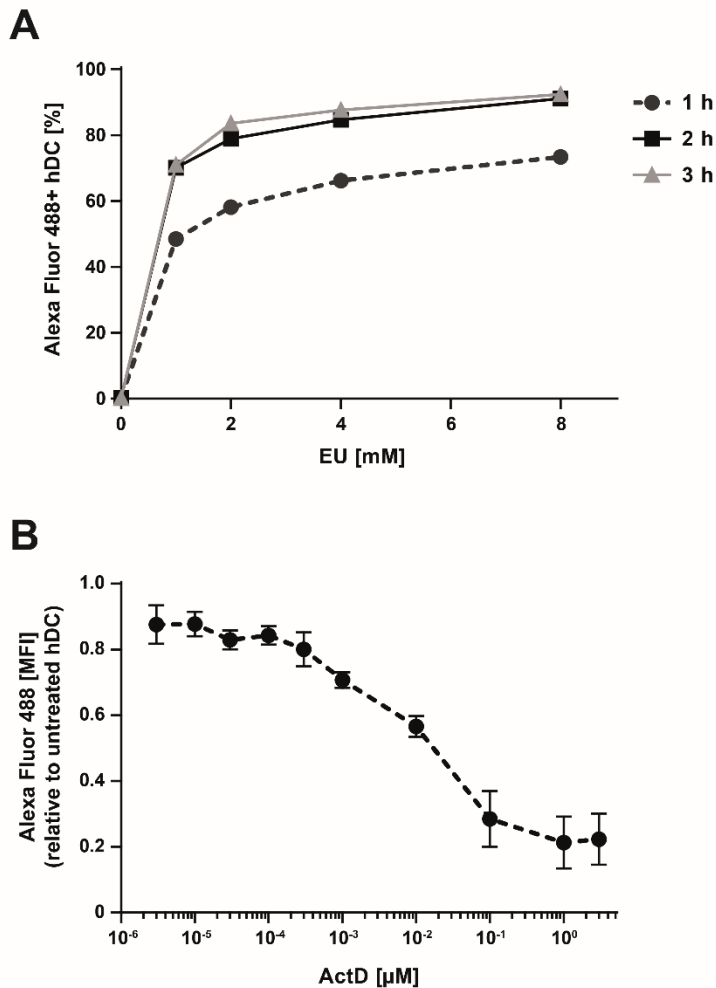
## **Analysis of inhibition of transcription**

For determination of the efficiency of inhibition of transcription hDCs were treated with different concentrations of 5-ethynyl uridine (EU) according to manufacturer's protocol. RNA was visualized via click-chemistry reaction by coupling the fluorescent dye Alexa Fluor 488 to EU using the Click-iT Nascent RNA Capture Kit. Subsequent visualization was performed by flow cytometric analysis of permeabilized and fixed cells using an Alexa Fluor 488-antibody (BD Biosciences).

## **Characterization of human iPSCs**

To stain iPSCs for the hESC surface marker TRA-1-81, cells were washed and incubated with TRA-1-81 live staining antibody (ReproCell) at a final concentration of 2.5 ng/ml for 30 min at 37 °C. After the incubation, cells were washed again and analyzed by fluorescence microscopy.

# Supplementary Figure 1



**Supplementary Figure 1: Transcription is efficiently inhibited in hDCs by treatment with Actinomycin D.** (A) Uptake and incorporation of fluorescent dye-labeled 5'-ethynyl uridine (EU) into RNA using click-chemistry. hDCs were treated with different concentrations of EU for 1 hr, 2 hr or 3 hr and after fluorescent dye coupling Alexa Fluor 488 positive hDCs were analyzed by flow cytometric (one experiment performed). (B) Transcription activity of cells treated with indicated concentrations of ActD for 5 hr. EU (8 mM) was added after 3 hr and cells were analyzed by flow cytometric for Alexa Fluor 488 expression after fluorescent dye coupling. Mean fluorescence intensity (MFI) of Alexa Fluor 488 positive hDCs as compared to untreated control cells is shown (four independently performed experiments).

# Supplementary Table 1

sample	time period of selection	half-life (rel. to LIB)
LIB	-	1.00
Rn1	24 h	0.91
Rn2	48 h	1.02
Rn3	48 h	0.87
Rn4	72 h	2.51
Rn5	72 h	5.97

**Supplementary Table 1: Comparison of half-lives during the selection process.** Half-lives of d2eGFP RNA expression shown in Fig. 1B were calculated from fitted one-phase decay curves and analyzed relative to the starting mRNA-library (LIB). The time period of selection after electroporation for round (Rn) 1-5 is also displayed

## Supplementary Table 2

Abbreviation	minimum length	median length	mean length	motive core area	flanking areas		Expression in hDC
	[nt]	[nt]	± SD [nt]		mean [%]	median [%]	
DNAJC4	113	216	199 ± 38	170	13	7	↗
FCGRT	121	189.5	195 ± 68	143	22	22	↗
MRS2	140	142	154 ± 21	142	7	1	↗
LSP1	134	156.5	175 ± 39	149	21	19	↗
CCL22	131	191	199 ± 50	155	28	21	↗
AES	136	200	202 ± 56	136	30	27	↗
PLD3	116	191	194 ± 42	190	17	20	↗
PTRF	163	172	179 ± 20	172	4	1	↗
mtRNR1	133	154	165 ± 32	142	12	10	n.a.
HLA-DRB4	163	249.5	241 ± 30	233	15	13	↗
CCDC124	103	175	208 ± 73	170	16	3	↗
PTMA	137	152.5	149 ± 7	142	6	4	↘
MYH9	135	167	218 ± 123	167	27	17	↗
CCL3	109	161	157 ± 47	109	43	42	↗
GLS	77	145	156 ± 58	126	57	55	↗

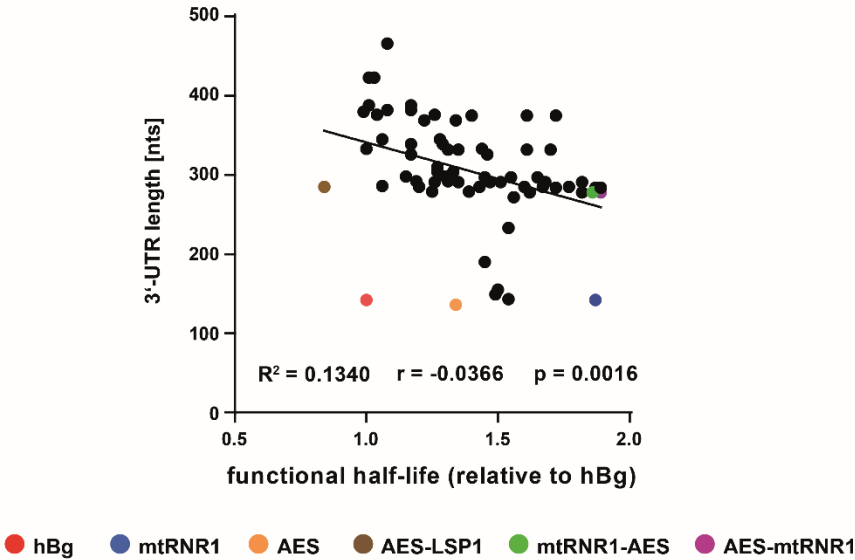
**Supplementary Table 2: Characteristics of redundantly retrieved sequences.** The mRNA origins to which each group of sequenced clones could be matched by BLAST alignment together with the minimum, median and mean length of identified sequences is provided. Analysis of flanking areas defined as sequence differences up- and downstream of the core area in percentage is shown as well. Respective genes are up- (↗) or downregulated (↘) in hDCs analyzed by NextBio (Illumina). nt, nucleotides; n.a., not applicable.

## Supplementary Table 3

Abbreviation	length [nt]	motive core area	
		sequence [5' → 3']	
DNAJC4	170	GGCCAGGCCCTTCCCTCTGCCCCCGGGTGTGAAGTCTAGCCCCATCCTGGTCCAATGCGCTTTGGTAGCTCCTTTCCAGCTGCCCGCCCGCCATGCCGCCCTTACTGCCCTGGCCGTGTGCCGGCTGTGGCCCGCAACCCTCCCTCCGGCTCCTCGGA	
FCGRT	143	TGCCCGTCTCACCAGACTGACTGCCTGCTGCTTTGCTACTGCCCGGGCCATGAGACTGACTTCCCACTGCTCTGCCTGCCTCTCCCCACTGCACTGGCACAGCCCCGCCCTTGCCGTGCTGATCCATTGCCGGTGTGACC	
MRS2	142	CTGCTGCCTGCTTCTTGTCTCCAGCACCATGGAATGCCTGCGCAGTTTACCCTGCCTCCTGCCCGCGCGGATGAGACTTCCCGGGGACGCTGTGTGCCCTGGCCTTGACGTGACCTCTGTGGTCTCCCGTTGCTGCCTTTCCAGCCAGACACCCGCCCGCCCTGGCTAAGAAGTTGCTTCTGTTGCCAGCATGACCTACCCTCGCCTCTTGATGCCATCCGCTGCCACCTCCTTTTGTCTCTGGACCCTTATGCCTCTCTGCCCTTCCACTCTGTGACCCC	
CCL22	155	GCCTTGGCTCCTCCAGGAAGGCTCAGGAGCCCTACCTCCCTGCCATTATAGCTGTCCCGCCAGAAGCCTGTGCCAATCTCTGCATTCCCTGATCTCCATCCCTGTGGGTGTCAACCTTGGTCACTCCGTGCTGTCACTGCCATCTCCCCC	
AES	136	CTGGTACTGCATGCACGCAATGTAGTGCCTTTCCCGTCTGGGTACCCCGAGTCTCCCCGACCTCGGTCCCAGGTATGCTCCACCTCCACCTGCCCACTCACCACTCTGTAGTTCCAGACACCTCC	
PLD3	190	CTGACAGCGTGGCAACGCCTGCCGCTGCTCTGAGGCCGATCCAGTGGGCAGGCCAAGGCCTGTGGGCCCCCGGGACCCAGGTGCTGTGGGTACGGTCCCTGTCCCGCACCCCGCTTCTGTCTGCCCATTTGGCTCCTCAGGCTCTCTCCCTGCTCTCCACCTTACTCCACCCCCAC	
PTRF	172	CTGACAGCGTGGCAACGCCTGCCGCTGCTCTGAGGCCGATCCAGTGGGCAGGCCAAGGCCTGTGGGCCCCCGGGACCCAGGTGCTGTGGGTACGGTCCCTGTCCCGCACCCCGCTTCTGTCTGCCCATTTGGCTCCTCAGGCTCTCTCCCTGCTCTCCACCTTACTCCACCCCCAC	
mtRNR1	142	CAAGCAGCAGCAATGCAGCTCAAAACGCTTAGCCTAGCCACACCCACGGGAAACAGCAGTGATTAACCTTTAGCAATAAACGAAAGTTAACTAAGCTATACTAACCCAGGGTTGGTCAATTTCTGTCAGCCACACCTTTTGCAAGATGAAACACTTCCCGCTTGGCTCTATTCTTCCACAAGAGAGACCTTCTCCGGACCTGGTGTACTGTTTCCAGCACTCTGCAGAAAATGTCTCCCTGTGGCTGCTCAGCTCATGCCTTTGGCCTGAAATGCCAGCATTGATGGCAGCCCTCATCTTCAAGTTTGTCTCCCTTACTAACGCTTCTGCTCCATGCATCTGTACTCTCC	
HLA-DRB4	233	CCTTGAGCTTGGAGTCTCCTCCTCCAGTAGGCGCTGCGTCTCCTTCTTACGTTCCAGTGGTCGAGGCGCGCTTCTCCTTCTCCTCTGCTGCTCCTTCTCATGACGTGTTGTGCTGCTCTCCAGTAGGCATCCTCCAGCTCCTTCTGCTTCTGGCATCA	

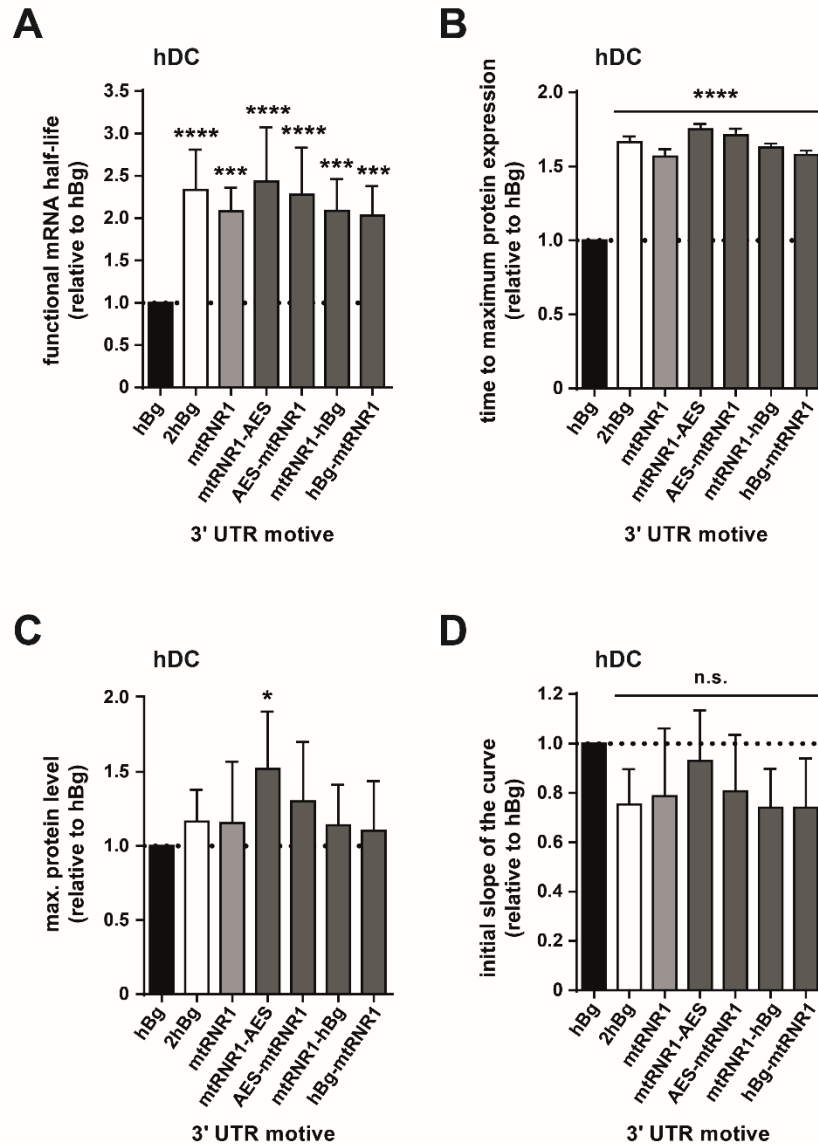
Supplementary Table 3: Sequences of most frequent motives recovered by the selection process. Sequences of identified core areas are displayed. nt, nucleotides.

# Supplementary Figure 2



**Supplementary Figure 2: The length of the 3' UTR correlates significantly with mRNA-stability.** Bioinformatical analysis of functional half-lives of mRNAs in correlation to the corresponding length of analyzed single or double 3' UTR motives. \*\* $p < 0.01$ ; r, Pearson correlation coefficient.

# Supplementary Figure 3

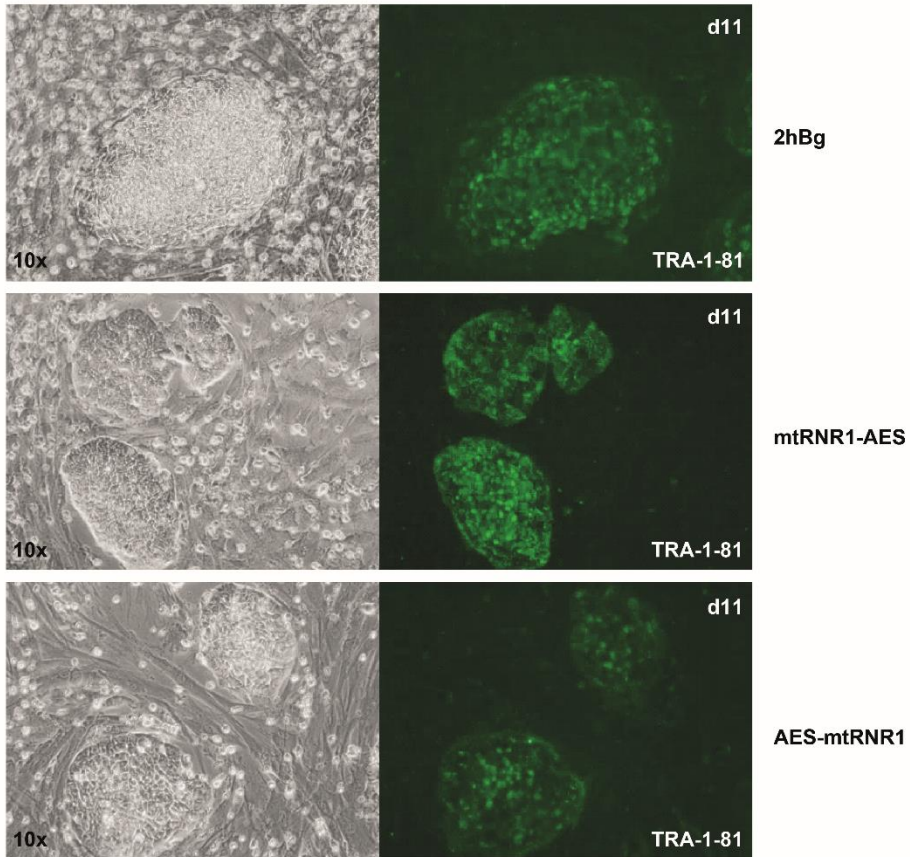


**Supplementary Figure 3: Analysis of relevant translational characteristics of mRNA deduced from protein decay kinetics in hDCs. (A-D)** Based on the data retrieved as described in Fig. 3A, functional mRNA half-life (A), the time period until the protein maximum is reached (B), maximum protein levels (C), and the initial slope of the curve (D) were calculated from protein decay kinetics and compared to luciferase mRNA with hBg as 3' UTR. One-way ANOVA, Dunnett's post-test; \*\*\*\*p<0.0001, \*\*\*p<0.001, \*\*p<0.01, \*p<0.05; n.s., not significant. (three independently performed experiments).

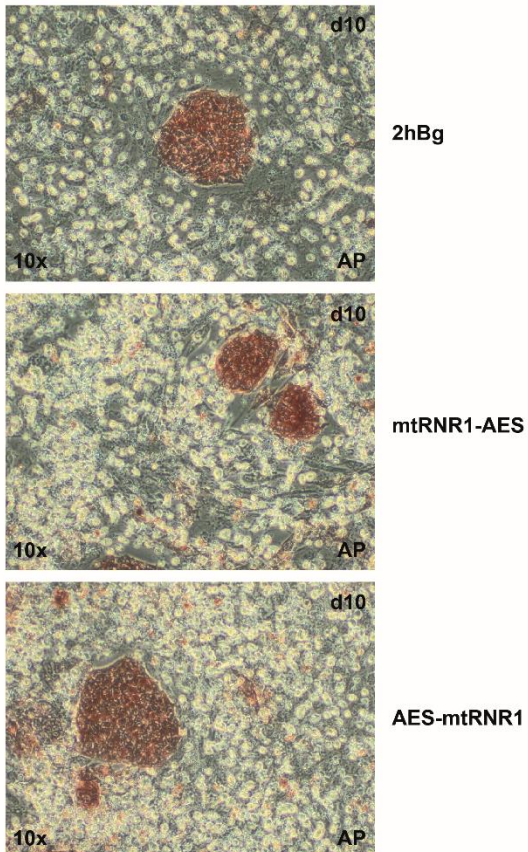


# Supplementary Figure 4

A



B



**Supplementary Figure 4: Pluripotency analysis of iPSC colonies obtained with mRNA tagged with mtRNR1 and AES 3' UTRs motives. (A and B) Pluripotency staining of HFF-derived iPSCs for hESC surface marker TRA-1-81 (A) and activity of AP (B). Representative images from stainings of iPSC colonies derived with four lipofections as described in Fig. 5 on day 10 or 11 (d10, d11) are shown.**